Supplementary Information (SI) for Journal of Materials Chemistry A.
This journal is © The Royal Society of Chemistry 2025

Supporting information for

Thiol Radical-Based Writable Colorimetric Indicators

Ziming Zhang, [a, b] *Xin Hong,* [a] *Weiming Xu,* [a] *Xinhong Xiong,* [b] *Jing Tu,* [b] *Luzhi Zhang,* [b*] *Jiaxi Cui* [a, b, *]

[a] Department: Institute of Fundamental and Frontier Sciences, University of Electronic Science and Technology of China, Chengdu 611731 (P. R. China).

[b] Yangtze Delta Region Institute (Huzhou), University of Electronic Science and Technology of China, Huzhou 313001 (P. R. China).

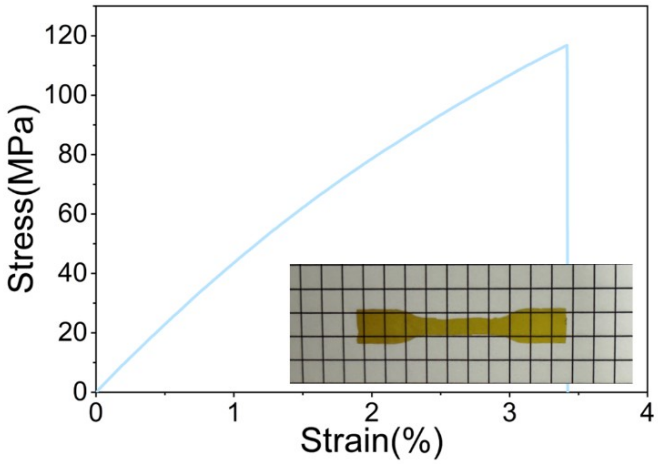

Figure S1. The thickness of the stretched spline is 0.05 mm, along with its mechanical properties.

To test mechanical properties, we stretched a film with a thickness of 0.05 mm. The maximum tensile strength and tensile strain are 116.7 MPa and 3.4% respectively, with a Young's modulus of 4.5 GPa, indicating high rigidity.

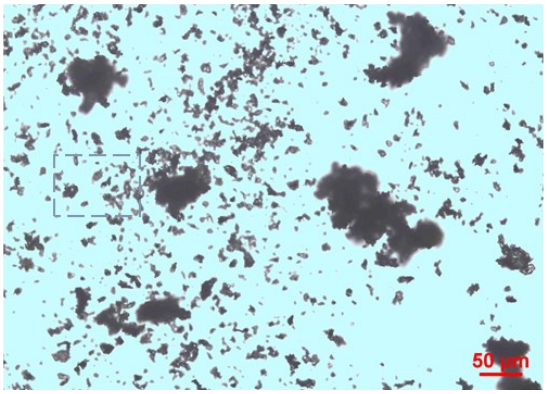

Figure S2. The size image of thiol radical polymer particles.

The approximate size of the particles depicted in the image ranges from 8 to 10 μm.

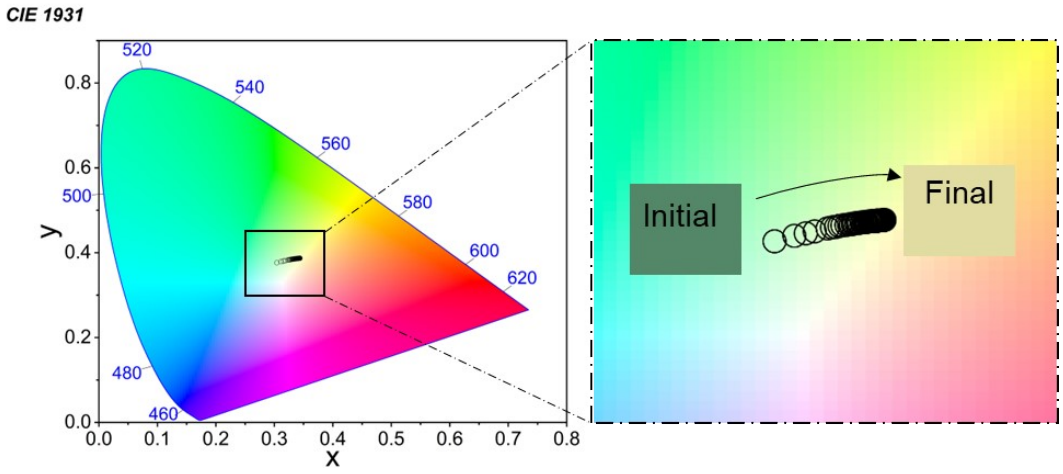

Figure S3. The color of thiol radical-anchoring polymer particles (TRAPs)undergoes changes over time due to the influence of temperature, humidity, oxygen, etc.

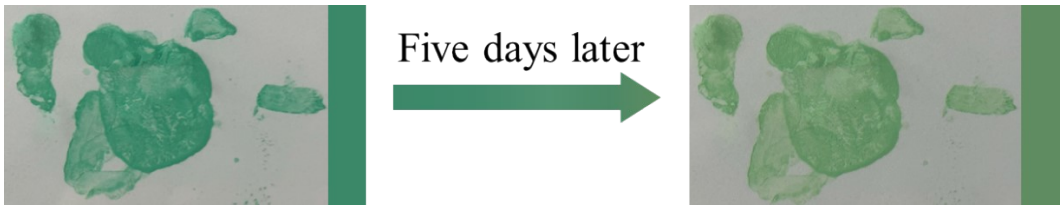

Figure S4. Color change of pattern from TRAPs after being placed in a glovebox for five days. The pressure, oxygen content, and water content in the glovebox were 0.22 mbar, 3 ppm, and 3 ppm, respectively, with the temperature maintained at room temperature (25°C).

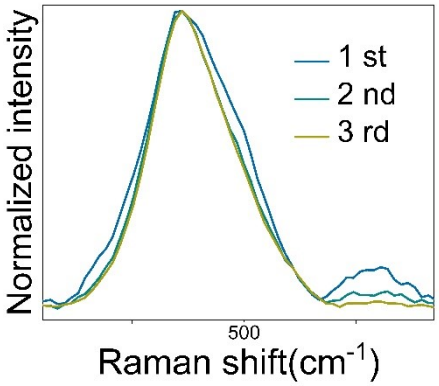

Figure S5. Raman spectra of TRAPs and their quenching products.

The characteristic signal representing radicals, with the peak at 564 cm^{-1} showing a decreasing trend, indicates that the content of radicals in TRAPs exhibits a decreasing trend over time.

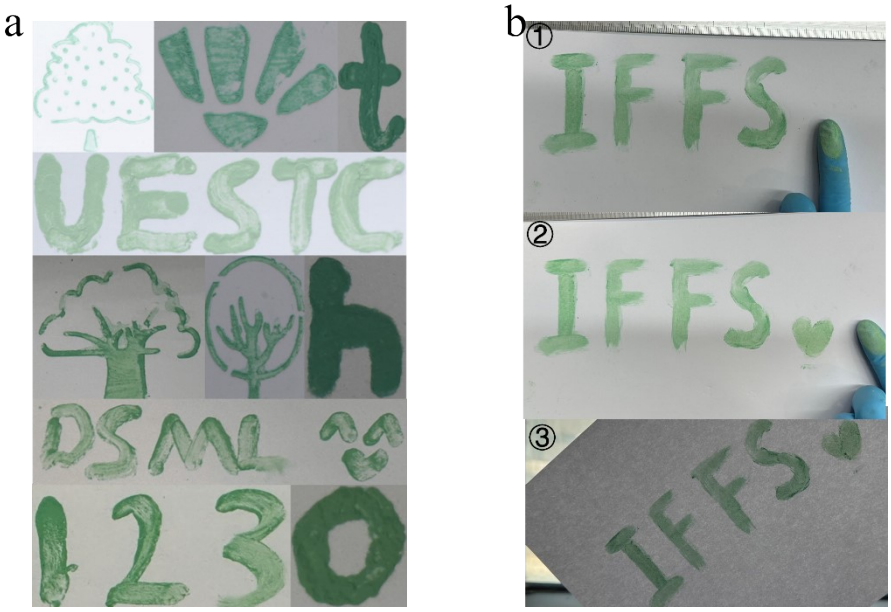

Figure S6. (a)Various patterns printed, written, or sprayed onto paper. (b) A solvent-free printing method was developed by simulating cold-press printing technology. At room temperature, TRAPs are impregnated and imprinted onto the paper surface, enabling direct writing.

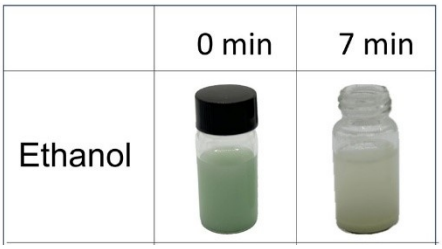

Figure S7. Color change images of TRAPs dispersed in ethanol and water after 7 minutes.

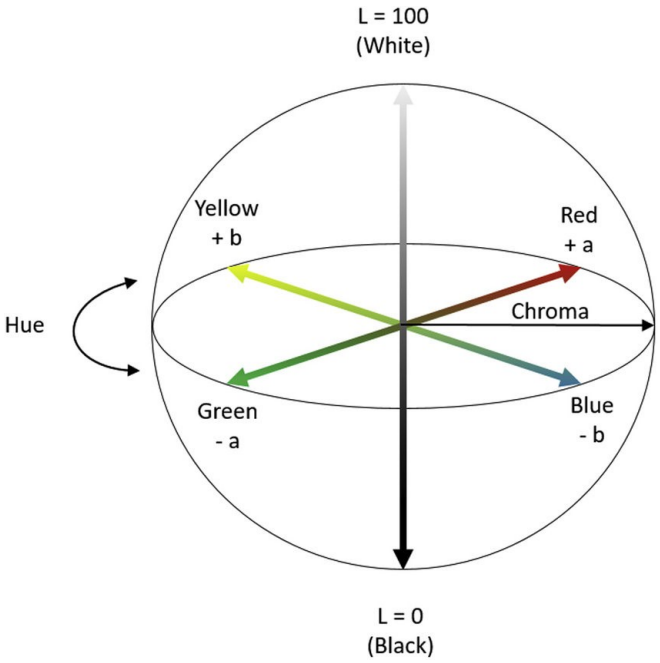

Figure S8. The CIELAB color space diagram.

a

Model	ExpDec1
Equation	y = A1*exp(-x/t1) + y0
Plot	50
y0	1.00744 ± 1.68927E-8
A1	-1.04365 ± 3.73184E-8
t1	28.31713 ± 2.22488E-6
Reduced Chi-Sqr	6.72E-14
R-Square (COD)	1
Adj. R-Square	1

b

Model	ExpDec1
Equation	y = A1*exp(-x/t1) + y0
Plot	70
y0	1.00001 ± 8.33005E-9
A1	-1.00001 ± 4.14262E-8
t1	15.75618 ± 1.08185E-6
Reduced Chi-Sqr	4.36E-14
R-Square (COD)	1
Adj. R-Square	1

c

Model	ExpDec1
Equation	y = A1*exp(-x/t1) + y0
Plot	100
y0	1 ± 6.4168E-9
A1	-1 ± 3.92128E-8
t1	11.77174 ± 7.26119E-7
Reduced Chi-Sqr	2.94E-14
R-Square (COD)	1
Adj. R-Square	1

d

Model	ExpDec1
Equation	y = A1*exp(-x/t1) + y0
Plot	10%
y0	1.00001 ± 8.33005E-9
A1	-1.00001 ± 4.14262E-8
t1	15.75618 ± 1.08185E-6
Reduced Chi-Sqr	4.36E-14
R-Square (COD)	1
Adj. R-Square	1

e

Model	ExpDec1
Equation	y = A1*exp(-x/t1) + y0
Plot	100%
y0	1 ± 7.78511E-9
A1	-1 ± 6.85451E-8
t1	5.65594 ± 5.86207E-7
Reduced Chi-Sqr	5.07E-14
R-Square (COD)	1
Adj. R-Square	1

Figure S9. Kinetic analysis of radical quenching under varying temperature and humidity conditions as reflected by changes in TRAPs' a^* value. (a) In 50℃ oven. (b) In 70℃ oven. (c) In 100℃ oven. (d) At 75℃ with 10% relative humidity (RH). (e) At 75℃ with 100% RH.

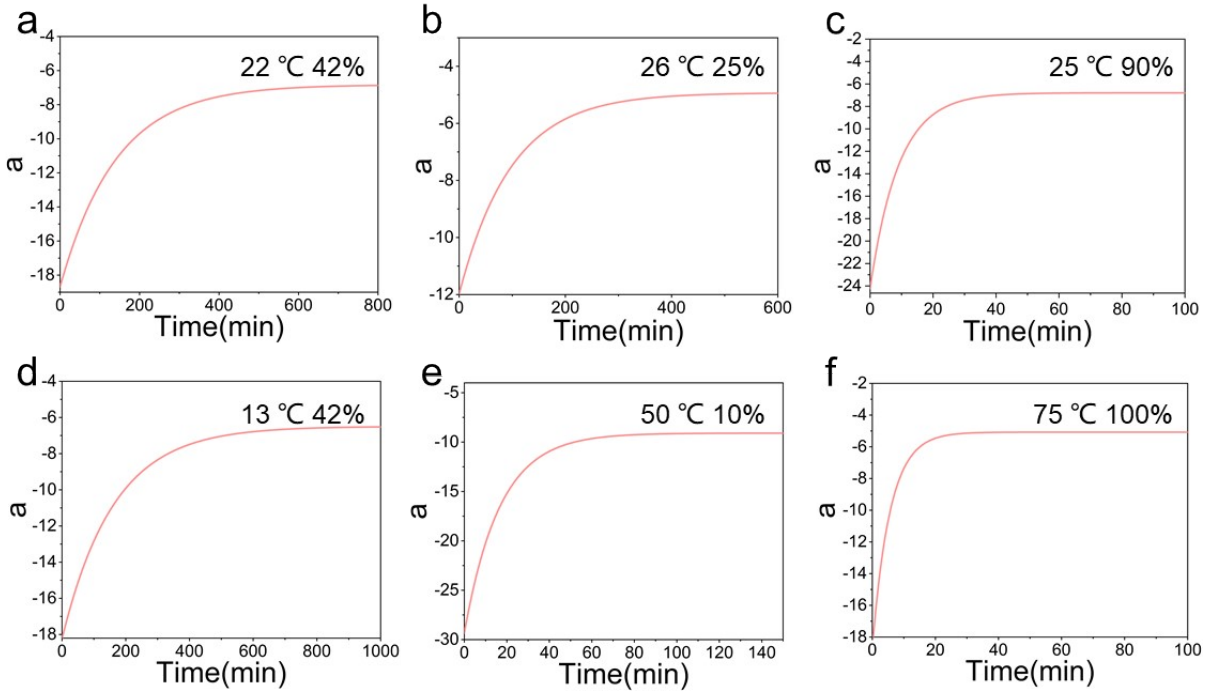

Figure S10. Changes in TRAPs ' a^* value were examined across various temperatures and relative humidities.

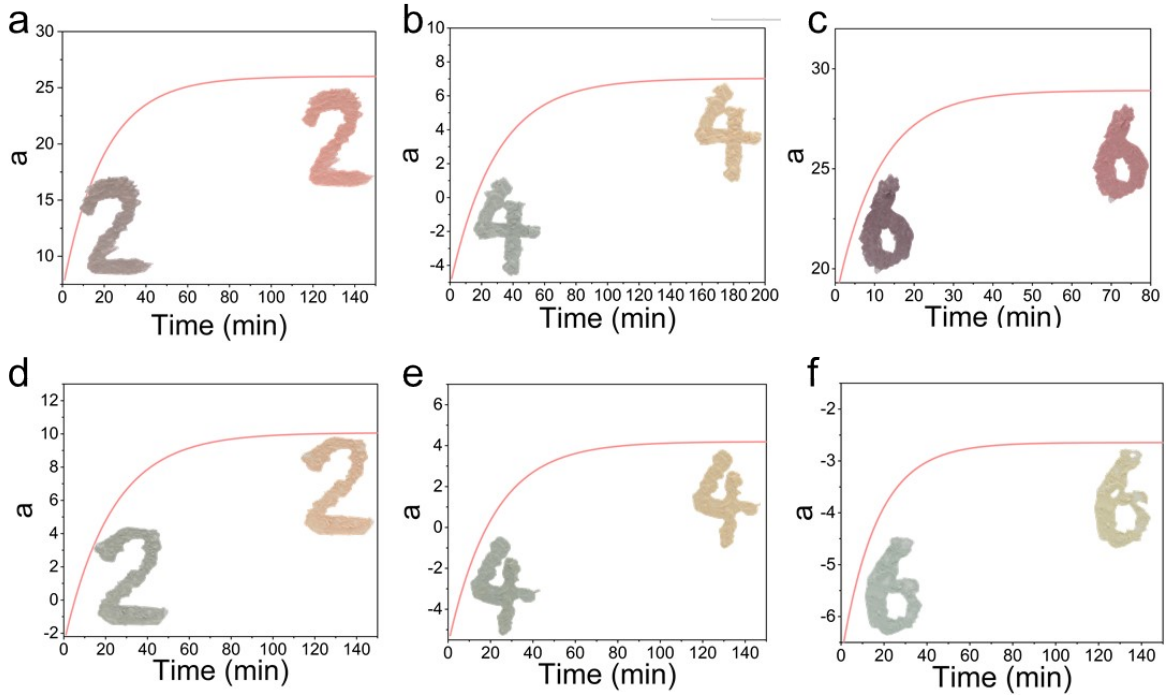

Figure S11. The changes in heterochromatic TRAPs under the condition of 26℃ and 25% relative humidity with different pigment concentrations. (a) Heterochromatic TRAPs with 0.024 wt% concentration of pigment red 254, (b) Heterochromatic TRAPs with 0.024 wt% concentration of red light C gold, (c) Heterochromatic TRAPs with 0.024 wt% concentration of 6B red pigment, (d) Heterochromatic TRAPs with 0.001 wt% concentration of pigment red 254, (e) Heterochromatic TRAPs with 0.001 wt% concentration of red light C gold.

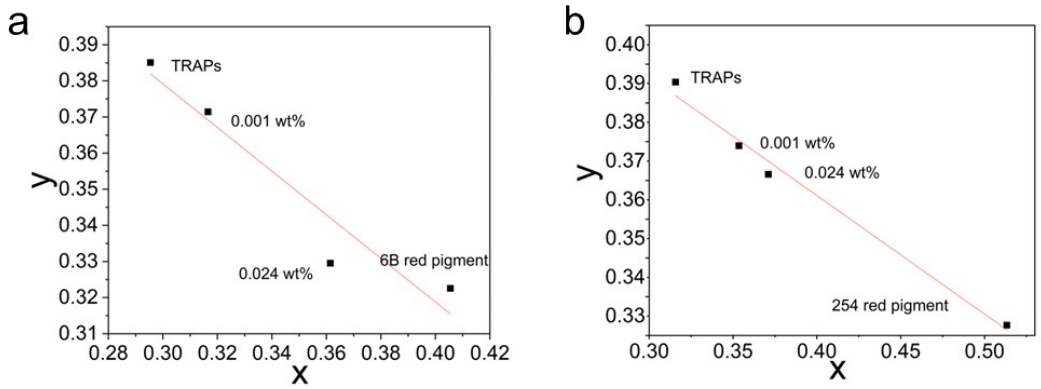

Figure S12. Positions of heterochromatic TRAPs with different pigment concentrations in the CIE chromaticity coordinates system, along with their fitted curves. (a) Coordinates for the series related to 6b red pigment. (b) Coordinates for the series related to pigment red 254.

Upon data fitting of the CIE chromaticity coordinates for heterochromatic TRAPs synthesized using 6b red and pigment red 254, the coefficient of determination (R^2) exceeded 0.92, with potential measurement errors contributing to the observed deviation. Notably, the color coordinates of heterochromatic TRAPs obtained by combining TRAPs with varying concentrations of the identical pigment were consistently positioned along the line connecting the pigment and TRAPs, adhering to the principles of the Grsassmann color law. Therefore, in accordance with the color mixing principles outlined by the Grsassmann color law, we possess the capability to formulate Heterochromatic TRAPs exhibiting any desired color.

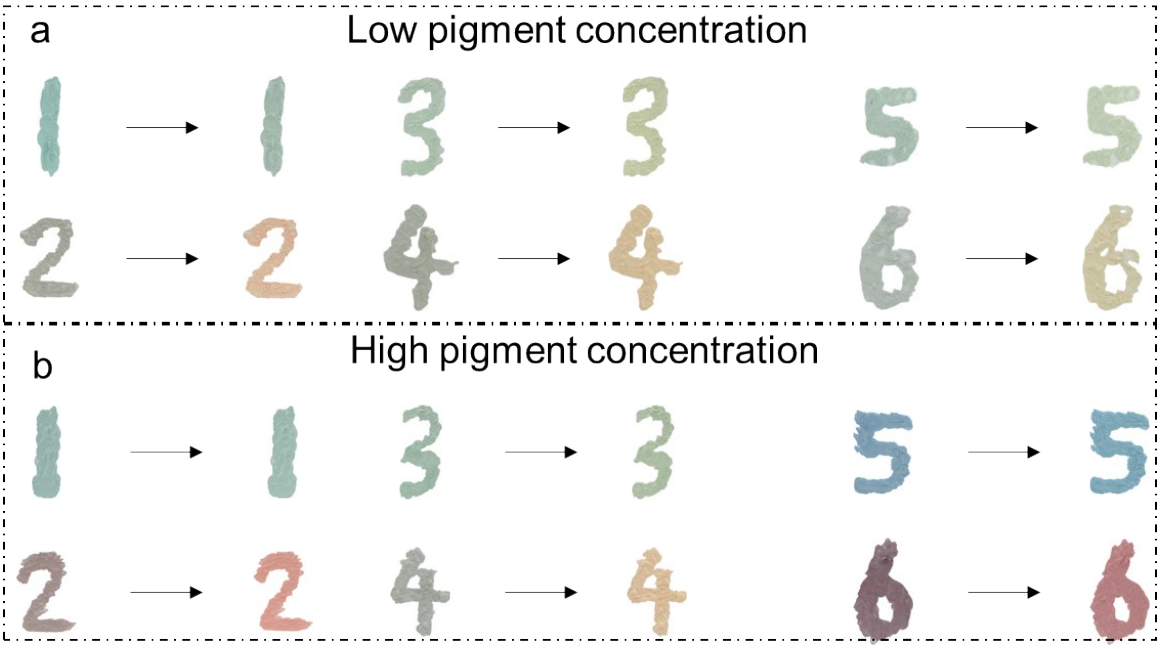

Figure S13. Colorimetry of heterochromatic TRAPs with various pigment levels at 26℃ and 25% relative humidity. (a) Heterochromatic TRAPs with 0.001 wt% pigment content. (b) Heterochromatic TRAPs with 0.024 wt% pigment content.

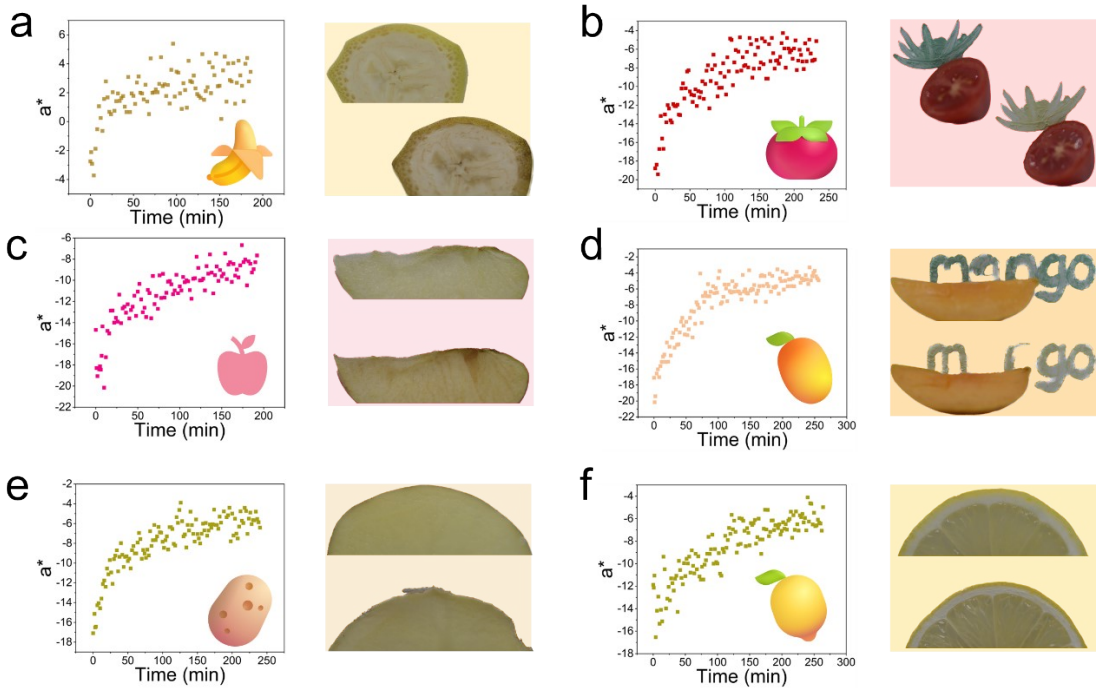

Figure S14. Different fruits and a* value of the color changes of TRAPs under conditions of 20.4℃ and 44% relative humidity in the atmospheric environment. (a) Banana, (b) Apple, (c) Pear, (d) Potato, (e) Tomato, (f) Mango, (g) Lemon, (h) Ice cream.

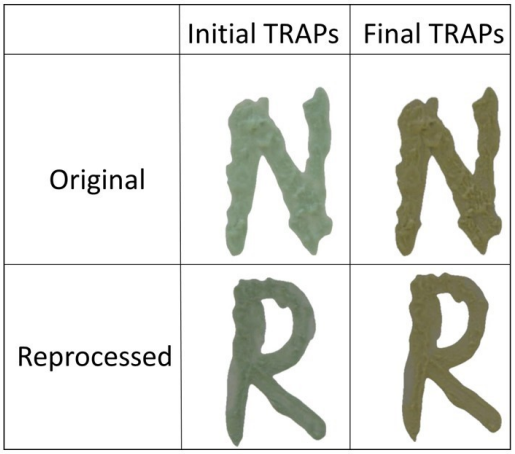

Fig. S15. Images of the original TRAPs and the reprocessed TRAPs used as indicators.